Methyl Group Internal Rotation Dynamics: Overtone Study of Gaseous Methylpyridine-2-αd_2 and -3-αd_2

A. Bergeat, D. Cavagnat,* C. Lapouge, and L. Lespade

Laboratoire de Physico-Chimie Moléculaire UMR5803, Université de Bordeaux I, 351 cours de la Libération, F-33405 Talence, France

Received: April 14, 2000; In Final Form: June 21, 2000

Conventional infrared absorption and Raman spectroscopy have been used to record the vapor phase spectra of methylpyridine-2-αd_2,6-d_1, methylpyridine-2-αd_2, and methylpyridine-3-αd_2,-d_4 in the $\Delta v_{CH} = 1-4$ regions. The spectra are analyzed with a theoretical model that takes into account, in the adiabatic approximation, the coupling between the internal rotation of the methyl group and the methyl CH stretching vibration. The principal parameters used in this model have been determined by ab initio calculations at the HF/6-31G** level of theory. A good agreement between experimental and calculated spectra is found. This indicates that this coupling is at the origin of the majority of the observed spectral profiles. A comparison of these results with those previously obtained for similar methylated molecules reveals that the change in type and size of the barrier to internal methyl rotation is at the origin of significant spectral differences. These changes are particularly important for methylpyridine-2-αd_2, revealing that the methyl group experiences increasingly different internal dynamics with increasing energy. These spectral changes can be well explained by the deformation of the effective internal rotation potential in the vibrational excited states. The overtone spectra of the aryl CD stretching of methylpyridine-3-αd_2,-d_4 have also been studied.

Introduction

The azines related to benzene through the substitution of one or more CH fragments by nitrogen atoms form the basic structure of numerous alkaloids and biological molecules of practical and theoretical interest. An understanding of the relationship between structure and biological properties of these compounds thus offers a fascinating and open area of research.[1]

Some studies have been reported on electronic distributions and resonance energies of these compounds compared with those of analogous benzenes.[2] Curiously, however, given the effect that conformation has on physical, chemical, and biological properties and processes, the conformational analysis of substituted azines has received scant attention, even for the simplest ones, the methylpyridines. Only a few previous studies have been devoted to the theoretical[3−5] and spectroscopic[6−13] study of these compounds. Among the latter, three works[10,11,13] are related to investigations of high excited vibrational states. Indeed, a study of the overtone spectra allows one to access additional information about detailed molecular structures and to characterize both intramolecular dynamics and related phenomena, such as unimolecular reactions and internal vibrational energy redistribution (IVR).

In addition to their application in fine organic syntheses (for example that of vitamin PP), the three methylpyridine derivatives, α-picoline (2-methylpyridine), β-picoline (3-methylpyridine), and γ-picoline (4-methylpyridine), present the particularity of possessing a large amplitude, very anharmonic motion (the methyl internal rotation) governed in the gas phase by intramolecular forces. This motion is quasifree in gaseous picolines, with barriers increasing from γ-picoline ($V = 4.7$ cm^{-1})[14] to α-picoline ($V = 91$ cm^{-1}).[15] Such an internal rotation is strongly coupled with many other vibrational motions, particularly with the methyl CH stretching vibrations.[9,11,16,17] The conformation-dependent CH vibrators thus constitute a unique probe for obtaining detailed microscopic information about the structure and internal dynamics of the material. As shown for similar molecules, the complex features observed in fundamental infrared and Raman spectra of the methyl CH stretching vibrations are conserved in the excited states but are often perturbed by the presence of strong CH stretch−bend Fermi resonance phenomena, leading to internal vibrational energy redistribution (IVR).[16−24]

A previous study of monohydrogenated toluene and γ-picoline has shown that both molecules exhibit almost the same spectral profiles, the only differences being essentially related to differences in electronic anharmonicity.[11] To complete this work, we are here examining β-picoline and α-picoline to analyze the effect of the environment of the methyl group and of the correlated symmetry on structure and on internal dynamics. Indeed, the symmetry of the potential of internal rotation of the CH_3 group decreases from 6-fold in the case of toluene and γ-picoline to 3-fold for the two other picolines. Furthermore, the relative position of the methyl group and of the N atom in the pyridine cycle is closer, particularly for α-picoline. We have again considered the CHD_2 derivatives, which offer simpler methyl CH stretching spectral features, generally little troubled by Fermi resonance phenomena, at least in the first overtone spectra.[11,20]

I. Experimental Section

1. Synthesis and Spectra. The isotopic derivatives (methylpyridine-2-αd_2,6-d_1, methylpyridine-2-αd_2, and methylpyri-

* Author to whom correspondence should be addressed. Fax: (+33) 556848402. Telephone: (+33) 556846360. E-mail: dcav@morgane.lsmc.u-bordeaux.fr.

10.1021/jp001414h CCC: $19.00 © 2000 American Chemical Society
Published on Web 09/15/2000

dine-3-αd_2,-d_4, denoted α-picoline-d_3, α-picoline-d_2, and β-picoline-d_6, respectively, in the following) were synthesized and purified according to the procedure described in ref 9. The isotopic purity, as determined by mass spectrometry, is 95%. The products were transferred under vacuum into different measurement cells.

Raman spectra (3250−80 cm^{-1}) were recorded with an OMARS 89 spectrometer equipped with a liquid-N_2-cooled CCD EGG detector (1024 diodes, grating 1800 grooves per mm, slits 100 Im × 2.35 cm^{-1}) and a Spectra Physics 2017 argon ion laser (514.5-nm beam at 4 W) providing exciting radiation. The diffusion light was recorded at 90° with a polarization filter. The spectra were recorded with a cylindrical Pyrex cell equipped with two windows tilted at the Brewster angle for multiple reflections at 333 K under equilibrium pressure (68 mmHg for α-picoline and 40 mmHg for β-picoline). The resolution was 1 cm^{-1}.

The FTIR spectra (12 000−900 cm^{-1}) were recorded with a Biorad FTS-60A Fourier transform infrared spectrometer (the sources were a quartz lamp and a glowing bar; KBr and quartz splitters were used; the detectors were DTGS or a Si diode). The gas cells were equipped with CaF_2 windows. For the range 3000−900 cm^{-1}, a homemade cell with a pathlength of 10 cm was used. The gas was at room temperature at equilibrium pressure (11.4 mmHg for α-picoline and 6 mmHg for β-picoline). The resolution was 0.5 cm^{-1}.

For the other IR spectra (12 000−3000 cm^{-1}), an Infrared Analysis long path cell (36 × 0.15 m = 5.4 m) was used and heated at 340 K with the gas at equilibrium pressure (90 mmHg for α-picoline and 54 mmHg for β-picoline). The resolution was 2 cm^{-1}.

The CH stretching Raman and IR spectra are similar for the two deuterated α-picolines. However, the methylpyridine-2-αd_2 product unfortunately contains an impurity because of the synthesis procedure that interferes with the CH stretching Raman spectrum of the α-picoline. Moreover, the signal-to-noise ratio of the IR spectra was better for methylpyridine-2-αd_2 than for methylpyridine-2-αd_2,6-d_1. Thus, it was decided to present the Raman spectrum of α-picoline-d_3 and the IR spectra of α-picoline-d_2.

The spectra of the perhydrogenated derivatives have also been recorded under the same experimental conditions and will be analyzed in a forthcoming paper.

2. Method of Calculation. All of the calculations were performed with the Gaussian 92 program at the Hartree−Fock level using the 6-31G** basis set.[25] Energy calculations have also been done by the MP2/6-31G** method with the addition of electronic correlation via a second-order Moller−Plesset perturbation. Vibrational frequencies were obtained by analytically determining second derivatives of the energy with respect to geometry distortions.

The previous study demonstrated that higher theory and basis set levels increased the calculation time considerably but did not significantly improve the accuracy of the calculated values, especially considering that we are particularly interested in the variations of the geometrical parameters.[11] The geometry of each molecule has been optimized for several values of the methyl group rotation angle θ, the aromatic ring being constrained to be planar. This approximation gives an error in the energy calculations of less than 1 cm^{-1}. As ab initio frequencies are always overestimated at the HF level, they have been scaled by factors 0.911 for ν_{CH}, 0.921 for ν_{CD}, and 0.9 for the other vibrations, as was done previously.[11]

II. Theoretical Approach

The theoretical approach has been well described in other articles,[9,11,16,20] so it is briefly recalled here. The coupling of the fast molecular vibrations to the much slower internal rotation motion of the methyl group is explicitly taken into account.

In a first approximation, the internal rotation motion can be described by a Hamiltonian of the form

$$\frac{H_r(\theta)}{hc} = \frac{\partial}{\partial\theta}B_\nu(\theta) + \frac{\partial}{\partial\theta}V_0(\theta) \qquad (1)$$

where θ is the internal rotation coordinate, $V(\theta)$ the rotational potential energy such that $V_0(\theta) = V_3/2[1 + \delta_3 \cos(3\theta)] + V_6/2[1 + \delta_6 \cos(6\theta)]$ [V_i and $\delta_i = \pm 1$ (i = 3 or 6) are calculated or fixed to the values determined by microwave spectroscopy[15]], and $B_\nu(\theta)$ the reduced rotational constant of the methyl rotor. $B_\nu(\theta) = B_e(\theta) - \alpha(\nu + {}^1/_2)$ varies with θ and with the vibrational quantum number ν. $B_\nu = h/(8\pi^2\mathbf{I}_{red}c)$, where $\mathbf{I}_{red}$ is the reduced inertia momentum, i.e., $\mathbf{I}_{red} = \mathbf{I}_\alpha(\mathbf{I}_a - \mathbf{I}_\alpha)/\mathbf{I}_a$ where $\mathbf{I}_a$ is the principal inertia momentum of the molecule, which is almost collinear with the methyl rotation axis and I_α is the CHD_2 inertia momentum, calculated from the internuclear distances determined by the ab initio calculations.[26,27] The calculated dependence of B on θ was found to be negligible (<0.006), with a variation in B_e equal to 0.01, causing no visible change in our low-resolution spectra. For the same reason, the effect of α, difficult to determine until $\Delta\nu = 4$, is also neglected.

The coupling of the vibrational and large-amplitude motions is modeled by the total Hamiltonian $\mathbf{H}_T = \mathbf{H}_{v-r} + \mathbf{H}_r$, which is solved in the adiabatic approximation. The total wave function is written as a product of two wave functions $\varphi(q_i,\theta)$, which describes the fast vibrational motions q_i and depends slowly on θ, and $\psi(\theta)$, which describes the much slower internal rotation. The Schrödinger equation can thus be separated into two equations, one describing the molecular vibrations (q_i) for each θ value, and the other describing the large amplitude motion, where the vibrational energy $e(\theta)$ acts as an additional potential.

$$\begin{aligned} H_{v-r}(q_i,\theta)\,\varphi(q_i,\theta) &= e(\theta)\,\varphi(q_i,\theta) \\ [H_r(\theta) + e(\theta)]\psi(\theta) &= E\psi(\theta) \end{aligned} \qquad (2)$$

The vibrational energy $e(\theta)$ acts as an additional potential for the rotational motion. Then, the effective potential of the rotational motion in the ground vibrational state is

$$V_{eff}(\theta,\upsilon{=}0) = V_0(\theta) + {}^1/_2\sum_i e_i(\theta)$$

with ${}^1/_2\Sigma_i e_i(\theta)$, the zero-point vibrational energy (ZPVE) of the $(3N - 7)$ vibrations other than the methyl rotation. ZPVE is calculated with corrected ab initio calculated vibration frequencies.

The effective potential of the rotational motion in the υ excited CH stretching state is

$$V_{eff}(\theta,\upsilon) = V_{eff}(\theta,\upsilon{=}0) + e_{CH}(\theta)$$

As discussed in a previous paper,[11] in the absence of strong perturbations due to Fermi resonance couplings, the CH stretching of the CHD_2 methyl group can be considered as independent of all vibrational motions other than the internal rotation. It is then well-described by Morse potential energy functions. The vibrational energy can thus be approximated by

$$e_{CH}(\theta) = \upsilon\varpi_{CH}(\theta) + \upsilon(\upsilon + 1)\chi(\theta) \qquad (3)$$

where $\varpi_{CH}(\theta)$ is the calculated CH stretching harmonic frequency and $\chi(\theta)$ its anharmonicity.

The energies and the wave functions of the internal rotational states corresponding to the ground vibrational state and to the v excited CH stretching vibrational level are calculated by solving the Schrödinger equations of motion with the effective potentials in a basis set of 85 free rotators. The CH stretching overtone spectra are then reconstructed by adding the CH transitions calculated between the energy levels of the two potentials $V_{eff}(\theta,0)$ and $V_{eff}(\theta,v)$ separated by an energy corresponding to the more stable equilibrium conformation.

The infrared intensity of these transitions between the two states $|0,N> \rightarrow |v,N'>$ (respectively the Nth and N'th internal rotational levels in the ground and excited states of CH bond stretching) is given by

$$\mathbf{I}_{|0,N\rangle\rightarrow|v,N'\rangle} = P[\int\int \varphi^*_{v}(q,\theta)\, \Psi^*_{vN'}(\theta)\, \mu(q,\theta)\, \varphi_0(q,\theta)\, \Psi_{0N}(\theta)\, dq\, d\theta]^2 \quad (4)$$

where $P = \exp[-(E_{0,N} - E_{0,0})/kT]$ is the Boltzmann factor and $\mu(q,\theta)$ the dipole moment function.

The dipole operator is decomposed along the three inertial axes of the molecule x, y, and z (where xz determines the molecular plane with z collinear with the CC methyl−ring bond and y perpendicular to the molecular plane, Figure 1). The infrared intensity is the result of the combination of the three contributions $\mu_x(q,\theta)$, $\mu_y(q,\theta)$, and $\mu_z(q,\theta)$.

The dipole moment function is approximated as a Taylor series expansion in the internal CH stretching displacement coordinate q about the equilibrium geometry. The dipole moment derivatives $\mu_j'^i(\theta)$ ($j = x$, y, or z), given by $\mu_j'^i(\theta) = (1/i!)(\partial^i/\partial q^i)\mu_j(q,\theta)|_e$, are calculated up to the fourth order by fitting ab initio dipole moment surfaces for different values of the internal motion coordinate. These surfaces are constructed by displacing the CH/CD stretching coordinates q from their equilibrium position and keeping the rest of the molecule at its optimized geometry, as described in ref 11.

Because $\varphi(q,\theta)$ depends slowly on θ (adiabatic approximation) and because, for each θ value, the mode intensities inside each polyad are supposed to come from the CH bond stretching overtones, the relation in eq 4 can be written

$$\mathbf{I}_{|0,N\rangle\rightarrow|v,N'\rangle} = P \sum_{j=1}^{3}[\sum_{i=1}^{4}\int \psi^*_{vN'}\, \mu'^i_j(\theta)\, c_j(\theta)\, \psi_{0N}\, d\theta \int \varphi^*_{v}(q,\theta)\, q^i \varphi_0(q,\theta)\, dq]^2 \quad (5)$$

The second integral corresponds to the matrix elements over the Morse oscillator wave functions (used to describe the very anharmonic CH vibrators) and the power of the coordinate (Table 1 of ref 11); the $\mu_j'^i(\theta)$ are the dipole moment derivatives along the axis j; and $c_z(\theta) = 1$, $c_x(\theta) = \cos(\theta)$, and $c_y(\theta) = \sin(\theta)$. The calculated molecular dipole moments are 1.94 D for the α-picoline, with $\mu_a = 0.81$ D and $\mu_b = 1.76$ D (very close to the measured values[15] $\mu_a = 0.72$ D and $\mu_b = 1.71$ D), and 2.50 D for the β-picoline, with $\mu_a = 1.42$ D and $\mu_b = 2.06$ D.

The interaction between the internal motion and the rotation of the molecule as a whole is neglected. The effect of the rotation of the entire molecule is taken into account by convoluting each transition by the corresponding asymmetrical top vibration−rotation profile (A-, B-, or C-type corresponding to μ_z, μ_x, or μ_y, respectively). Picolines are indeed asymmetrical tops ($I_a = 147.4$, $I_b = 318.8$, and $I_c = 460.9 \times 10^{-40}$ g cm^2 measured[15] and $I_a = 144.0$, $I_b = 314.6$, and $I_c = 453.5 \times 10^{-40}$ g cm^2 calculated for the perhydrogenated α-picoline and $I_a = 144.0$, $I_b = 321.2$, and $I_c = 460.2 \times 10^{-40}$ g cm^2 calculated for the perhydrogenated β-picoline), with the greatest principal moment of inertia (I_c) perpendicular to the molecular plane and the smallest one (I_a) almost collinear with the methyl top rotation axis (Figure 1). These values, modified by deuteration are calculated to be $I_a = 147.2$, $I_b = 342.2$, and $I_c = 479.2 \times 10^{-40}$ g cm^2 for α-picoline-d_2 and $I_a = 169.5.0$, $I_b = 369.6$, and $I_c = 531.6 \times 10^{-40}$ g cm^2 for β-picoline-d_6, both studied here. The profiles are characterized by the value of the PR separation and the Q branch intensity (for α-picoline, ΔPR = 13.6, 8.8, and 12.0 cm^{-1} and $I_Q = 19\%$, 0%, and 29% for the A, B, and C types, respectively, and for the β-picoline, ΔPR = 12.8, 8.8, and 12.8 cm^{-1} and $I_Q = 19\%$, 0%, and 30% for the A, B, and C types, respectively). To calculate the spectra, we have assigned to each transition its corresponding vibration−rotation theoretical profile calculated in the harmonic approximation from rotational constants determined by ab initio calculations.[28,29] These

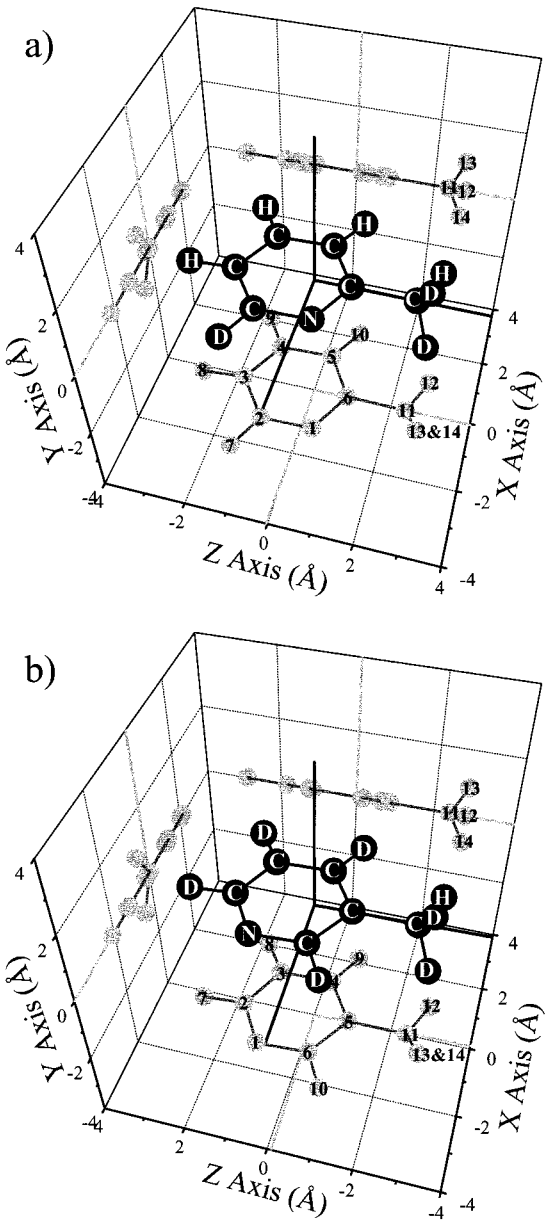

Figure 1. (a) α-Picoline-d_3 and (b) β-picoline-d_6 geometries and inertial axes with their projections onto the three planes.

TABLE 1: Geometric Parameters of α- and *β*-Picoline[a,b]

	α-picoline			*β*-picoline		
	minimum values (for θ)	maximum values (for θ)	relative variation	minimum values (for θ)	maximum values (for θ)	relative variation
C_6N	1.3215 (60°)	1.3259 (0°)	0.33	1.3220 (60°)	1.3172 (0°)	0.36
C_2N	1.3190 (0°)	1.3241 (60°)	0.39	1.3179 (60°)	1.3227 (0°)	0.36
C_3C_2	1.3798 (60°)	1.3844 (0°)	0.34	1.3810 (0°)	1.3857 (60°)	0.34
C_4C_3	1.3823 (0°)	1.3868 (60°)	0.33	1.3807 (60°)	1.3855 (0°)	0.35
C_5C_4	1.3785 (60°)	1.3834 (0°)	0.35	1.3845 (0°)	1.3894 (60°)	0.35
C_6C_5	1.3893 (0°)	1.3943 (60°)	0.37	1.3874 (60°)	1.3923 (0°)	0.35
H_7C_2	1.0769 (60°)	1.0771 (0°)	0.02	1.0764 (0°)	1.0766 (60°)	0.02
H_8C_3	1.0744	1.0744	0.00	1.0748	1.0748	0.00
H_9C_4	1.0761	1.0761	0.00	1.0767 (0°)	1.0772 (60°)	0.05
$H_{10}C_{(5\text{ or }6)}$	1.0747 (0°)	1.0754 (60°)	0.07	1.0775 (60°)	1.0783 (0°)	0.07
$C_{11}C_{(6\text{ or }5)}$[c]	1.5065 (0°)	1.5078 (60°)	0.09	1.5089 (60°)	1.5096 (0°)	0.05
$H_{meth}C_{11}$	1.0809 (180°)	1.0869 (80°)	0.54	1.0838 (0°)	1.0867 (90°)	0.27
C_3C_2N	123.77 (60°)	123.78 (15°)	0.01	123.00 (0°)	123.03 (60°)	0.02
$C_4C_3C_2$	117.66 (0°)	117.69 (300°)	0.03	118.34 (60°)	118.37 (0°)	0.03
$C_5C_4C_3$	118.90 (60°)	118.95 (0°)	0.04	119.58 (0°)	119.59 (60°)	0.01
$C_6C_5C_4$	118.98 (0°)	119.03 (60°)	0.04	116.61 (0°)	116.64 (60°)	0.02
H_7C_2N	115.91 (60°)	116.04 (0°)	0.11	116.37 (0°)	116.48 (60°)	0.09
$H_8C_3C_2$	120.62 (0°)	120.67 (60°)	0.05	120.40 (60°)	120.47 (0°)	0.05
$H_9C_4C_3$	120.64 (60°)	120.69 (0°)	0.05	120.20 (0°)	120.27 (60°)	0.06
$H_{10}C_{(5\text{ or }6)}C_{(4\text{ or }5)}$[c]	120.80 (0°)	120.93 (60°)	0.11	119.59 (0°)	119.73 (60°)	0.12
$C_{11}C_{(6\text{ or }5)}C_{(5\text{ or }4)}$[c]	121.78 (0°)	121.81 (60°)	0.81	121.77 (60°)	122.57 (0°)	0.66
$H_{12}C_{11}C_{(6\text{ or }5)}$[c]	110.09 (105°)	111.76 (0°)	1.51	111.12 (60°)	111.26 (105°)	0.13
$H_{13}C_{11}C_{(6\text{ or }5)}$[c]	109.72 (60°)	110.07 (105°)	0.32	111.06 (0°)	111.23 (45°)	0.15
$H_{14}C_{11}C_{(6\text{ or }5)}$[c]	110.07 (0°)	111.70 (105°)	1.47	111.14 (45°)	111.25 (15°)	0.10
energy[d]	−285.748 392 276 (0°)	−285.748 014 412 (180°)		−285.744 998 640 (180°)	−285.744 755 562 (0°)	

[a] Bond lengths (in Å) and angles (in degrees). [b] Maximum and minimum values for the methyl rotation angle θ (in degrees) and the relative variations (in %). [c] The first set of numbers is for α-picoline, and the second set is for *β*-picoline. [d] Energy (in hartrees).

profiles are convoluted by a Lorentzian function mixed with a Gaussian function with a width adjusted for each overtone.

For the Raman intensity, the transition operator is the polarizability associated with the CH bond. The first isotropic $\partial\bar{\alpha}(\theta)/\partial r_{CH}$ and anisotropic $\partial\bar{\gamma}(\theta)/\partial r_{CH}$ polarizability derivatives have been calculated, for each θ value, from the molecular polarizability tensor derivatives calculated with Gaussian 92.[30] The depolarization ratio ρ value for the CH bond, calculated to be between 0.29 and 0.32, is in good agreement with the experimental value (see section III.2). The CH stretching is thus mainly isotropic ($\rho < {}^3/_4$).

The isotropic Raman intensities are calculated with a relation similar to that used for the infrared intensities (4), replacing $\mu(q,\theta)$ by the mean isotropic polarizability $\bar{\alpha}(q,\theta)$. This polarizability is also expanded as a Taylor series in the CH stretching displacement. Here, we have only considered the first term of the transition operator development, which is a good approximation because of the preponderant value of the first Morse coefficient at $\Delta v = 1$. Assigning a Lorentzian profile to each transition simulates the isotropic Raman spectrum.

III. Results

1. Geometry Optimizations and Frequency Calculations. The geometry of α- and *β*-picolines is shown in Figure 1 for a methyl rotation angle $\theta = 0°$ (the origin of the methyl rotation angle is taken to be when the CH bond of the CHD_2 methyl group is in the aromatic ring plane and at the opposite side of the nitrogen atom).

The geometry of each molecule has been optimized for each θ value, the aromatic ring being constrained to be planar. There is no experimentally determined structure available to compare our results, but such a comparison done in a previous article for toluene[11] has shown that the regularity of experimental values was retrieved. Furthermore, our calculated parameters are in good agreement with those recently published and calculated using different ab initio bases.[13]

For both α- and *β*-picolines, the equilibrium conformation of the methyl group is not staggered, as in toluene or *γ*-picoline,[11] but eclipsed with a CH bond pointing toward the N atom for the *β* isomer ($\theta = 180°$) and on the opposite side for the α isomer ($\theta = 0°$). The calculated potential energy of the internal rotation V_0 has a 3-fold symmetry with rotational barriers of 51.3 and 82.9 cm^{-1} for *β*- and α-picoline, respectively (Table 2). MP2/6-31G** calculations lead to slightly higher values of 57.7 and 91.9 cm^{-1} for *β*- and α-picoline, respectively. These values are very similar to those previously calculated by Henry et al. in the 6-31+G** (52.3 cm^{-1} for *β* and 113.8 cm^{-1} for α) and 6-311++G** bases (59.4 cm^{-1} for *β* and 111.6 cm^{-1} for α).[13] They are in good agreement with the experimental value determined by Dreizler et al. by microwave spectroscopy for α-picoline, $90.4/2[1 - \cos(3\theta)] - 4.1/2[1 - \cos(6\theta)]$.[15] In the following, we have introduced the experimental value of the potential in the calculations for α-picoline and, for *β*-picoline, as no experimental value is available, the MP2 value that appears to be the closest to the experimental value for α-picoline.

The internuclear distances and the angles present only small variations with the rotation of the methyl group, except those of the methyl group (Table 1). The angle between the methyl group and the aromatic carbons [$C_{11}C_6C_5$ (α) or $C_{11}C_5C_4$ and $C_{11}C_5C_6$ (*β*)] is larger than the usual 120° because of a weak van der Waals repulsion between the methyl and aromatic CH bonds. When the methyl CH bond rotates from 0° to 60°, the $C_{11}C_6C_5$ angle and the length of the C_6C_5 and $C_{11}C_6$ bonds increase for α-picoline, whereas the $C_{11}C_5C_4$ angle and the length of the C_5C_6 and $C_{11}C_5$ bonds decrease for *β*-picoline, the minimum value of these parameters corresponding to the equilibrium conformation of the methyl group in each isomer.

TABLE 2: Parameters Involved in the Calculation of the Spectra of Methylpyridine-2-αd_2 (α-Picoline), Methylpyridine-3-αd_2,-d_4 (β-Picoline), and Methylpyridine-4-αd_2,-d_4 (γ-Picoline)

		γ-picoline[h]	β-picoline	α-picoline
V_0[a]	V_3	0.0[h] *or* 0.0[k]	51.4[i] or 57.7[j] ($\delta_3 = 1$)	82.9[i] *or* 90.4[k] ($\delta_3 = -1$)
	V_6	2.1[h] *or* 4.7[k] ($\delta_6 = +1$)	−1.3 ($\delta_6 = -1$)	0.3[i] *or* −4.1[k] ($\delta_6 = -1$)
ZPVE[b]	E_1	0.0	−0.75	−2.40
	E_2	15.0	10.50	17.70
	E_3	0.0	−0.85	8.70
	E_4	0.2	0.30	0.30
$\boldsymbol{r}_{CH}$[c]	r_0	1.0848	1.08514	1.0844
	$r_1 \times 10^{-3}$	0.0	0.13	2.8
	$r_2 \times 10^{-3}$	−3.30	−2.9	−4.4
	$r_3 \times 10^{-3}$	0.0	−0.06	−0.1
	$r_4 \times 10^{-3}$	0.16	0.16	0.3
ϖ_{CH}[d]	ϖ_0	2950.8	2945.0	2955.8
	ϖ_1	0.0	−1.7	−34.7
	ϖ_2	32.0	32.5	49.8
	ϖ_3	0.0	0.70	0.1
	ϖ_4	−2.0	−1.7	−2.4
χ_{CH}[e]	χ_2	1.5	1.5	1.5
B_e[f]		3.406	3.329	3.343
$\partial\bar{\alpha}/\partial r_{CH}$[g]	α_0		4.041	4.601
	α_1		−0.009	−0.020
	α_2		−1.455	−1.423
	α_3		−0.035	−0.038
	α_4		−0.006	−0.012

[a] V_0, rotational barrier (in cm^{-1}). $V_0(\theta) = V_3/2[1 + \delta_3 \cos(3\theta)] + V_6/2[1 + \delta_6 \cos(6\theta)]$. [b] Zero-point vibrational energy (in cm^{-1}). ZPVE $= E_0 + {}^1/_2\Sigma_i[E_i \cos(i\theta)]$. [c] Internuclear distance (in Å). $r_{CH} = r_0 + {}^1/_2\Sigma_i[r_i \cos(i\theta_0)]$. [d] CH stretching harmonic frequency (in cm^{-1}). $\varpi_{CH} = \varpi_0 + {}^1/_2\Sigma_i[\varpi_i \cos(i\theta_0)]$. [e] Anharmonicity (in cm^{-1}). $\chi_{CH} = \chi_0 + {}^1/_2\chi_2 \cos(2\theta)$. [f] B_e, reduced rotational constant (in cm^{-1}). [g] Mean molecular polarizability derivative (in 10^{-30} C^2 m J^{-1}). $(\partial\bar{\alpha}/\partial r_{CH}) = \alpha_0 + {}^1/_2\Sigma_i[\alpha_i \cos(i\theta_0)]$. [h] Reference 4. [i] Ab initio Calculations 6-31G**. [j] Ab initio Calculations MP2/6-31G**. [k] Microwave experiment, Refs 14 and 15.

The values of the variation of the methyl CH bond with the rotation angle are very similar to those calculated for γ-picoline or toluene,[11] but this variation no longer has a strict 2-fold symmetry, especially for α-picoline (Table 2). The maximum CH length difference is 5.9×10^{-3} Å for α-picoline and 3.0×10^{-3} Å for β-picoline. The length of the CH bond is a maximum at $\theta \approx 90°$ (1.0859 Å) for β-picoline and at $\theta \approx 80°$ (1.0869 Å) for α-picoline. As for γ-picoline or toluene,[11] this could be explained by a hyperconjugation effect with the π electronic cloud of the aromatic ring. When the CH bond is in the ring plane, the van der Waals repulsion is the strongest, and the CH bond is shorter. For β-picoline, the methyl CH bond length is essentially the same (1.0838 Å) in both positions ($\theta \approx 0°$ or 180°), but for α-picoline, because of the close neighbor of the N atom, the methyl CH bond is longer at $\theta \approx 0°$ (1.0837 Å) than at $\theta \approx 180°$ (1.0809 Å). Contrary to what is often assumed,[1] the attractive interaction between the methyl group hydrogen and the in-plane lone-pair electrons of the nitrogen atom appears to be weaker than the attraction exerted by the π electronic cloud of the pyridine ring. This can explain the equilibrium conformation of the methyl group in α-picoline. The preference for the conformation at $\theta \approx 180°$ (rather than that at $\theta \approx 0°$) for β-picoline can correspond to a minimum in the aryl CH−alkyl CH interaction.

The calculated and scaled vibrational frequencies are reported in Tables 3 and 4. They are compared with the infrared and Raman experimental frequencies recorded in the gas phase. The assignment of fundamentals is proposed, with the PED (potential energy distribution) indicating a majority participation of the internal coordinates. It can be noted that the CH stretching mode of the CHD_2 methyl group is a pure mode (PED > 99%).

The principal parameters used in our model are issued from these ab initio calculations and are displayed in Table 2 with those found for γ-picoline[11] for comparison. Contrary to what was previously encountered,[11,16,17,20] the conformational dependence of these parameters during the internal rotation no longer has strict 2-fold symmetry. Indeed, if the case of β-picoline is very similar to that of γ-picoline with a mainly $\cos(2\theta)$ dependence, the $\cos\theta$ contribution is almost half of the $\cos 2\theta$ contribution for the α-picoline variation, showing the disturbing effect of the nearness of the N atom. The harmonic CH stretching frequency ϖ_{CH} presents a variation related to that of the CH bond length with a mean frequency shift of 11.1 cm^{-1} (α) and 11.8 cm^{-1} (β) for a CH bond length variation of 10^{-3} Å, in good agreement with the values found for numerous similar molecules.[11] The mean value of the anharmonicity of the methyl CH stretching can be estimated from the relative positions of the peaks at $\Delta\nu = 1-4$ at 60 ± 1 cm^{-1}, with a conformational dependence $\Delta\chi_{CH} = (1.5 \pm 0.5)\cos(2\theta)$.

The effective potentials of the methyl internal rotation corresponding to the ground vibrational level and to the first excited state of CH bond stretching, the energy levels of internal rotation, and the probability of their corresponding wave functions are shown in Figure 2 for both β-picoline-d_6 and α-picoline-d_3 (or α-picoline-d_2, whose ZPVE is very close to that of α-picoline-d_3). In the ground vibrational state, the most stable equilibrium conformation corresponds to $\theta = 115°$ for the α-picoline and 60° for β-picoline. The other equilibrium conformation at $\theta = 0°$ for α-picoline and 180° for β-picoline has a higher energy [+11.9 cm^{-1} (α) and +8.7 cm^{-1} (β)]. In the CH stretching excited states, because of its vibrational part, the effective potential barrier becomes even higher at $\theta = 180°$ for α-picoline (96 cm^{-1} at $\nu = 0$ to 361 cm^{-1} at $\nu = 4$) and at $\theta = 0°$ for β-picoline (64.7 cm^{-1} at $\nu = 0$ to 207.2 cm^{-1} at $\nu = 4$) when the vibrational energy increases (Figure 2). In the meantime, for both molecules, the most stable equilibrium conformation tends to be displaced at $\theta = 90°$, and the less stable one tends to disappear. The intermediate barrier is progressively shifted toward $\theta = 0°$ (α) and $\theta = 180°$ (β), and its height (68.8 cm^{-1} for α-picoline at $\theta = 0°$ and 48.6 cm^{-1} for β-picoline at $\theta = 120°$ at $\nu = 0$) decreases to 0 at $\nu = 4$. The effective potential becomes thus an almost 2-fold potential

TABLE 3: Vibrational Modes in Gaseous Methylpyridine-2-αd_2-6d_1 (α-Picoline)[a]

α-picoline						
min	max	min scaled	max scaled	exp IR	exp Raman	assignment[b] (PED%)
−49	52	−44	46			τ_{methyl}(75) τ_{ring}(15)
213	216	191	194		186.1	γ_{ring}(88) τCH_{ring}(7)
342	352	308	317			$\delta C(N)CC_{methyl}$(75.5)
437	439	393	395			τ_{ring}(97)
494	502	445	452			τ_{ring}(65) γCH_{ring}(28)
568	576	511	519		528.8	δ_{ring}(44) νCC_{methyl}(25)
678	680	610	612		621.8	δ_{ring}(70) γCH_{ring}(21)
719	745	647	671			τ_{ring}(64) $\gamma CH/D_{ring}$(24)
834	837	751	753		761.2	δ_{ring}(29) νCC_{methyl}(26) ν_{ring}(19)
837	844	753	759		775.7	τ_{ring}(40) γCH_{ring}(36) γCD_{ring}(23)
872	916	785	824			τ_{ring}(36) γCH_{ring}(31) γCD_{ring}(24.5)
925	964	832	868			r_{methyl}(48) δCD_{ring}(30) ν_{ring}(17)
987	995	888	895			$\gamma CH/D_{ring}$(53) τ_{ring}(34) $_{rmethyl}$(12)
994	1011	895	910		915.7	δCD_{ring}(36) ν_{ring}(28) $_{rmethyl}$(20)
1033	1054	930	949			γCH_{ring}(59.5) τ_{ring}(34)
1091	1093	982	984		986	δ_{ring}(48.5) ν_{ring}(38)
1126	1127	1014	1014		997.4	γCH_{ring}(52) δ_{ring}(48)
1156	1162	1041	1046			$\delta CD_{2methyl}$(87)
1179	1183	1061	1065	1050	1050	ν_{ring}(87) δCH_{ring}(9)
1201	1202	1081	1082	1090	1089.4	ν_{ring}(51) δCH_{ring}(45)
1229	1252	1106	1127		1115.4	ν_{ring}(38) δCD_{ring}(18) δCH_{ring}(14)
1309	1321	1178	1189	1161.5	1161.9	δCH_{ring}(44) ν_{ring}(31) δCH_{methyl}(10)
1337	1374	1203	1237	1234	1230.5	δCH_{ring}(44) ν_{ring}(23) δCH_{methyl}(17)
1416	1425	1275	1283	1282	1276	δCH_{methyl}(99)
1429	1465	1286	1319	1315	1308	δCH_{methyl}(61) νCC_{methyl}(20)
1580	1589	1422	1431	1422	1418.2	δCH_{ring}(52) ν_{ring}(35)
1617	1623	1455	1461	1450		δCH_{ring}(46) ν_{ring}(37) νCC_{methyl}(10)
1771	1775	1594	1597	1591.3	1594.2	ν_{ring}(68.5) δCH_{ring}(19)
1797	1799	1617	1619			ν_{ring}(66.5) δCH_{ring}(20)
2325	2344	*2141*	*2159*	2154	2154	$\nu_s CD_{2methyl}$(98)
2400	2442	*2211*	*2249*	2255		$\nu_a CD_{2methyl}$(99)
2473	2475	*2278*	*2280*	2266.1	2262.3	νC_2D_7 (97)
3215	3290	**2929**	**2997**	2951/2962	2951/2962	νCH_{methyl}(99.1)
3345	3347	**3047**	**3049**	3014		νC_4H_9 (73) C_5H_{10}(17) C_3H_8(10)
3363	3369	**3064**	**3069**	3068	3068	νC_5H_{10} (67) C_3H_8(29)
3377	3378	**3077**	**3077**	3077.6	3076.1	νC_3H_8 (61) C_4H_9(23) C_5H_{10}(16)

[a] The scaled frequencies have been multiplied by 0.9, except the frequencies ν_{CH} in bold, by a factor 0.911 and the frequencies ν_{CD} in italic by a factor 0.921. [b] ν = bond stretching, δ = in plane angle bending, γ = out of plane angle bending, and τ = torsion.

with a higher barrier wall (at $\theta = 0°$ for β and at $\theta = 180°$ for α) and a wide lower one (at $\theta = 180°$ for β and at $\theta = 0°$ for α). For β-picoline, the difference between these two barrier heights is relatively constant as v increases ($\Delta E \approx 50$ cm^{-1}). For α-picoline, the repulsive effect of the nitrogen atom favors the increase of the height of the barrier at 180°, and this energy difference increases with v ($\Delta E \approx 222$ cm^{-1} at $v = 4$ and 292 cm^{-1} at $v = 6$).

2. Fundamental Methyl CH Stretching Spectra. *Raman Spectra.* The experimental and calculated vapor-phase Raman spectra of α-picoline-d_3 and β-picoline-d_6 in the fundamental CH stretching region are shown in Figure 3.

These spectra are essentially isotropic. The experimental depolarization ratio is difficult to measure because of the weakness and the bad signal-to-noise ratio of the I_{vh} signal. It can be estimated as <0.2, in good agreement with the calculated value (see section II). A comparison of the I_{vv} and I_{vh} Raman spectra shows that the anisotropic part gives only a wide, weak, unstructured feature and can be considered as a continuous baseline. Thus, only the isotropic CH stretching Raman spectra have been taken into account in the simulation.

To reconstruct these spectra, we have used the parameters of the internal rotation effective potentials in Table 2 (Figure 2). The intensities for the isotropic CH stretching Raman spectra have been calculated as explained in part II with the mean polarizability derivatives ($\partial\bar{\alpha}/\partial r_{CH}$) displayed in Table 2. These derivatives present the same variation with the methyl rotation angle θ for α- and β-picoline. The mean molecular polarizability for the entire molecule, $\bar{\alpha} = {}^1/_3(\alpha_{xx} + \alpha_{yy} + \alpha_{zz})$ determined from ab initio calculations is 9.9×10^{-40} C^2 m^2 J^{-1} for both α- and β-picoline.

Because of the localization of the wave functions in the potential wells, the transitions between the four or six first internal rotational levels in each vibrational state are intense. The transitions $|0,0> \rightarrow |1,0>$ and $|0,1> \rightarrow |1,1>$ correspond to a CH vibrator in a position close to the perpendicular position [around $\theta = 110°$ (α) and around $\theta = 65°$ (β)] (Figure 2). They give rise to the lowest-frequency peak in each spectrum, at 2951 and 2941 cm^{-1} for α- and β-picoline, respectively (Figure 3). The transition $|0,2> \rightarrow |1,2>$ corresponds to an in-plane CH vibrator position at $\theta = 0°$ for α-picoline and at $\theta = 180°$ for β-picoline and to the less intense feature at 2965 cm^{-1} for both compounds. The more intense band in each spectrum [at 2962 (α) and 2951 cm^{-1} (β)] corresponds to transitions between internal rotation levels in a more or less free-rotation regime. It can be noted that this free-rotation regime is reached sooner for β-picoline ($N = 6$, $v = 0$; $N' = 7$, $v = 1$) than for α-picoline ($N = 7$, $v = 0$; $N' = 11$, $v = 1$).

The calculated spectra are in good agreement with the experimental ones (Figure 3). A comparison of the experimental and scaled ab initio frequencies (Tables 3 and 4) reveals a frequency shift toward high energy for the CH stretching of

TABLE 4: Vibrational Modes in Gaseous Methylpyridine-3-αd_2-d_4 (β-Picoline)[a]

β-picoline						
min	max	min scaled	max scaled	exp IR	exp Raman	assignment[b] (PED%)
−48	46	−43	41			τ_{methyl}(70) τ_{ring}(23)
209	212	188	191		183.5	τ_{ring}(89) γCD_{ring}(7)
319	326	287	293			$\delta C(N)CC_{methyl}$(78)
401	402	361	362			τ_{ring}(97.5)
461	470	415	423			τ_{ring}(81) γCD_{ring}(12)
549	552	494	497		507	δ_{ring}(62) δCD_{ring}(16)
624	625	562	563			τ_{ring}(66) γCD_{ring}(33)
668	669	601	602		612	δ_{ring}(69) δCD_{ring}(21)
719	727	647	654			τ_{ring}(68) γCD_{ring}(28.5)
808	812	727	731		745	δCD_{ring}(30) δ_{ring}(25) νCC_{methyl}(22)
849	859	764	773		760	γCD_{ring}(54) τ_{ring}(26) r_{methyl}(20)
865	868	779	782			γCD_{ring}(61) τ_{ring}(39)
882	919	794	827		820	δCD_{ring}(73.5) ν_{ring}(19)
920	928	828	835			δCD_{ring}(54) ν_{ring}(20) r_{methyl}(23)
930	932	837	838			γCD_{ring}(81) τ_{ring}(18)
935	958	841	862		850	r_{methyl}(39) ν_{ring}(32) δCD_{ring}(21)
976	981	879	883		888	δCD_{ring}(67.5) ν_{ring}(13) δ_{ring}(12)
995	1035	895	931			γCD_{ring}(52) r_{methyl}(41)
1095	1096	985	986		990	δ_{ring}(49) ν_{ring}(26) δCD_{ring}(20)
1137	1142	1023	1028	1013.5	1010.4	δCD_{ring}(81)
1160	1162	1044	1046	1047	1048	$\delta CD_{2methyl}$(90)
1213	1219	1092	1097			ν_{ring}(89) δCD_{ring}(9)
1260	1279	1134	1152	1153.5	1153	νCC_{methyl}(36) ν_{ring}(23) δCD_{ring}(14)
1408	1424	1268	1282	1231	1230	δCH_{methyl}(63) ν_{ring}(22)
1427	1432	1284	1289		1285	δCH_{methyl}(100)
1473	1501	1326	1351	1337		δCH_{methyl}(35) ν_{ring}(34) δCD_{ring}(13)
1532	1536	1379	1383	1382	1382	ν_{ring}(51) δCD_{ring}(24) νCC_{methyl}(15)
1744	1747	1569	1572	1550.5	1550	ν_{ring}(75.5) δCD_{ring}(10)
1776	1778	1599	1600		1572	ν_{ring}(71.5) δCD_{ring}(12)
2325	2337	*2141*	*2152*	2152.6	2153	$\nu_s CD_{2methyl}$(98.5)
2402	2421	*2212*	*2230*		2190	$\nu_a CD_{2methyl}$(99)
2460	2464	*2265*	*2269*	2260.5	2268	νC_6D_{10}(87.5) C_2D_7(7.5)
2467	2468	*2272*	*2273*			νC_4D_9(38) C_3D_8(26.5) C_2D_7(26)
2477	2479	*2281*	*2283*	2272	2279	νC_4D_9(47.5) C_2D_7(46.5)
2504	2505	*2307*	*2307*	2293	2292	νC_3D_8(69) νC_2D_7(17) C_4D_9(10)
3212	3252	**2927**	**2962**	2951/2941	2951/2941	νCH_{methyl}(99.4)

[a] The scaled frequencies have been multiplied by 0.9, except the frequencies ν_{CH} in bold, by a factor 0.911 and the frequencies ν_{CD} in italic by a factor 0.921. [b] ν = bond stretching, δ = in plane angle bending, γ = out of plane angle bending, and τ = torsion.

the methyl group. As previously discussed[11] and demonstrated[31] for toluene, it is due to weak anharmonic coupling with methyl CHD_2 group bending overtones. This coupling becomes very strong for the CH_3 toluene derivatives and leads to a strong Fermi resonance perturbation.[31]

As expected, the spectra of the two molecules are very similar and, in every respect, resemble the spectra of γ-picoline-d_7 and toluene-d_7.[11] We can nevertheless note that the frequency difference between the two main peaks is only 11 cm^{-1} here instead of 13 cm^{-1} for toluene-d_7 and γ-picoline-d_7.[11] For these latter two molecules, the lower-frequency peak corresponds to a conformation of the CH methyl bond perpendicular to the ring molecular plane (with a consequently longer CH bond and lower CH stretching frequency), instead of a 60° tilted conformation for α-picoline-d_3 and β-picoline-d_6. This shows that the environment of the methyl group does not have a striking influence on the fundamental Raman spectra, but the increased barrier size and the lower symmetry of the hindering potential nevertheless have a tangible effect.

Infrared Spectra. The experimental and calculated infrared spectra of gaseous α-picoline-d_2 and β-picoline-d_6 in the fundamental CH stretching region are presented in Figures 4a and 5a, respectively.

The reconstruction of these spectra uses the same effective potential parameters as those used for the Raman spectra. Their intensities have been calculated as explained in part II with the dipole moment derivatives reported in Tables 5 and 6. The magnitude and the cos(2θ) variation of these dipole moment derivatives are very similar as those of toluene-d_7 and γ-picoline-d_7 (Tables 2 and 3 of ref 11). The intensity of each transition is obtained by summing the contributions of the three dipole moment components (μ_x, μ_y, and μ_z). These spectral contributions are also drawn in Figures 4a and 5a.

The infrared spectra of the fundamental methyl CH stretching region exhibit features similar to those of the Raman spectra, but with more complex profiles. The μ_y component of the dipole moment gives rise to a C-type band with an intense Q branch centered at 2951 cm^{-1} (α) and at 2941 cm^{-1} (β), essentially due to transitions involving a 110° (α) or 65° (β) tilted CH vibrator. The μ_x component of the dipole moment induces a B-type band centered at 2965 cm^{-1} for both compounds, essentially due to transitions involving a 0° (α) or 180° (β) in-plane CH vibrator. The μ_z component of the dipole moment generates an A-type band centered at 2962 cm^{-1} (α) and at 2951 cm^{-1} (β), essentially due to transitions involving a freely rotating CH vibrator. This latter contribution forms the major part of the intensity of the spectra. We can note that the frequencies of the "in-plane" CH rotator and of the free CH rotator are very close for α-picoline. Because of the high potential barrier at $\theta = 180°$ at $v = 1$ (151 cm^{-1}), the free-rotation regime is reached only for rotational levels with $N > 10$, and thus, the most intense "free-rotation" transitions

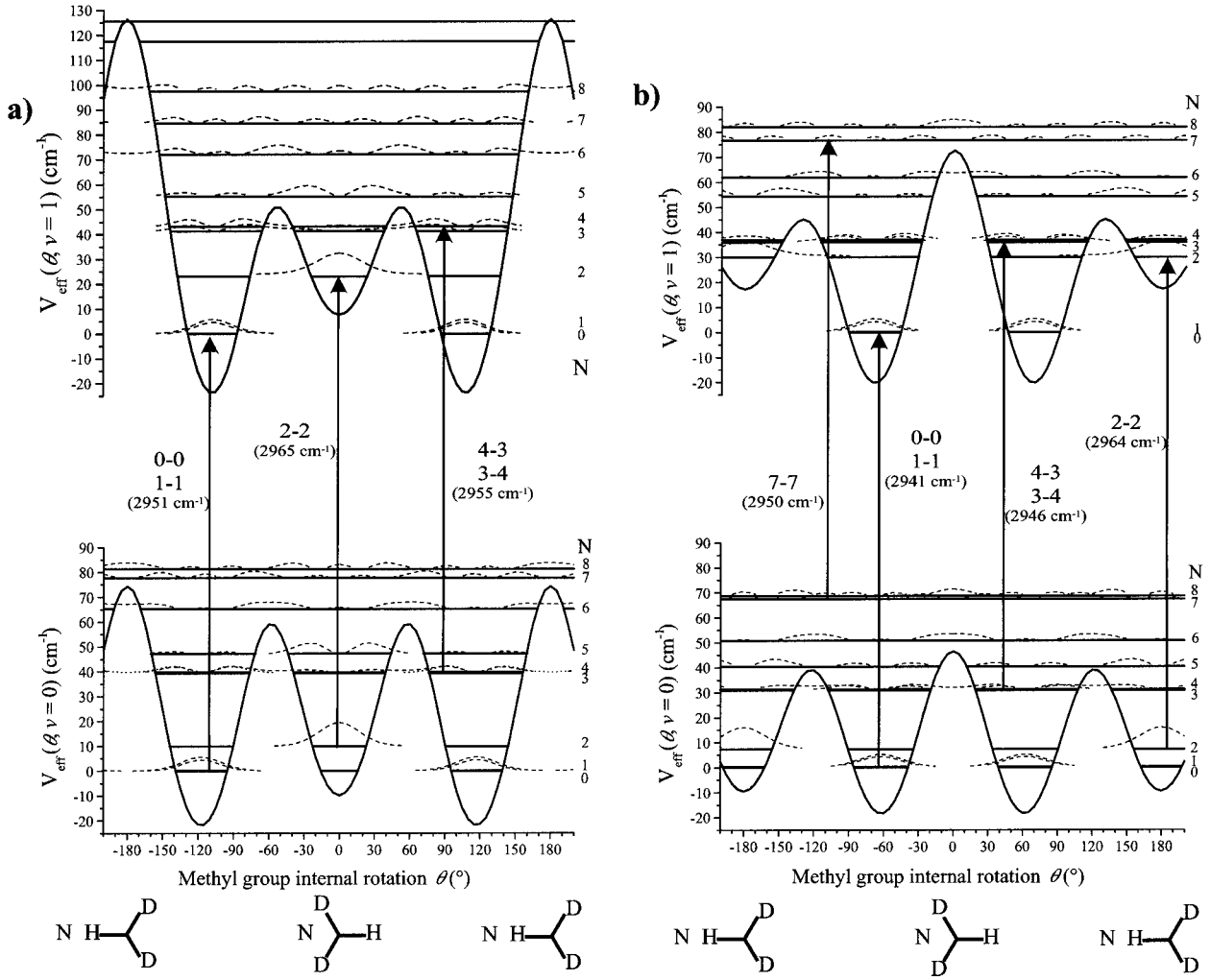

Figure 2. (a) α-Picoline-d_3 or α-picoline-d_2 and (b) β-picoline-d_6 effective potential energies of internal rotation (θ) in the ground and first excited CH stretching vibrational states.

correspond, in fact, to vibrators hindered between two extreme positions around $\theta = \pm 150°$ with a mean position at $\theta = 0°$.

Compared to the corresponding spectra of toluene-d_7 and γ-picoline-d_7,[11] we note that the Q branch due to the μ_y component of the dipole moment is better observed in the fundamental spectra of α-picoline-d_2 and β-picoline-d_6. This could be explained by the higher barrier height of these latter molecules in the ground vibrational state, which leads to the localization of a greater number of internal rotational level wave functions around the equilibrium conformation ($N = 0, 1, 3, 4$) (Figure 2).

Again, we observe a good fit of the experimental spectra with the calculated ones.

3. Overtone Methyl CH Stretching Spectra. The experimental and calculated infrared spectra of gaseous α-picoline-d_2 and β-picoline-d_6 in the CH stretching regions corresponding to $\Delta v_{CH} = 2-4$ are presented in Figures 4 and 5, respectively.

These spectra also present complex features. The methyl CH stretching overtone spectra have also been recorded for the perhydrogenated compounds and are in very good agreement with those published by R. Proos and B. Henry.[13] We noted that the CHD_2 spectra frequencies are shifted toward high energy, as expected from the now-well-known CH/CD interaction effect.[23,24] R. Proos and B. Henry[13] also report the vibrational overtone spectra of the H impurities of perdeuterated β-picoline. Their spectra compare well with those presented here but are largely perturbed by the numerous differently deuterated species present in the material, especially for the third overtone spectrum (Figure 8 of ref 13), making a precise analysis difficult.

β-Picoline. The first overtone spectrum of the methyl CH stretch of β-picoline-d_6 exhibits only a broad band centered at 5775 cm^{-1} with a weak Q branch emerging at 5760 cm^{-1} and two wings at 5816 and 5725 cm^{-1} (Figure 5b). This embedded feature, compared to that of toluene-d_7,[11] is due to the progressive increase and deformation of the effective potential in the excited vibrational states. As discussed above (part III.1), the depth of the intermediate well at $\theta = 180°$ decreases (down to 10 cm^{-1} at $v = 2$), whereas that of the principal well increases (up to 127 cm^{-1} at $v = 2$). The wave function of the internal rotational levels localized in this well at $\theta = 180°$ in the first excited vibrational state are now localized in the principal potential well. This gives rise to the intense transitions $|0,3> \rightarrow |2,2>$ and $|0,4> \rightarrow |2,3>$ around 5767 cm^{-1}, which fill in the gap between the free-rotator (5782 cm^{-1}) and the tilted-rotator (5758 cm^{-1}) peaks.

The two higher-energy overtone spectra exhibit patterns very similar to those of the corresponding spectra of toluene-d_7.[11,31] They exhibit three peaks at 8454, 8496, and 8541 cm^{-1} for $\Delta v = 3$ and 11032, 11083, and 11140 cm^{-1} for $\Delta v = 4$. These three peaks can again be related to the CH bond in a tilted conformation versus the molecular plane, in free rotation, and in an in-plane conformation. From $\Delta v = 3$, the effective excited-state potential tends to resemble that of toluene-d_7[11] at the same energy, with a potential well minimum shifted toward $\theta = 80°$

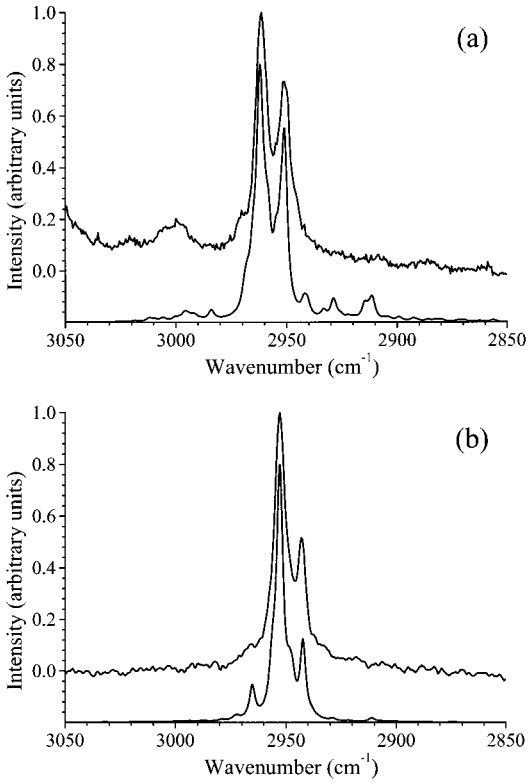

Figure 3. Experimental (top curve) and calculated (bottom curve) Raman spectra of (a) α-picoline-d_3 and (b) β-picoline-d_6.

(instead of 90°) and two potential barriers at $\theta = 0°$ and $\theta = 180°$, but with a barrier height difference of 50 cm^{-1} (instead of equal), a difference still small relative to the thermal energy of the molecule. These differences have no effect on the spectral profile of the high overtone spectra.

α-*Picoline.* The first overtone spectrum of the methyl CH stretch of α-picoline-d_2 presents two distinct bands centered at 5774 and 5806 cm^{-1}, with a lower frequency shoulder at 5738 cm^{-1} (Figure 4b). This feature appears different from that of toluene-d_7[11] and from that above observed of β-picoline-d_6 (Figure 5b). Indeed, the deformation of the effective potential in the excited vibrational state is still stronger than for β-picoline. Most of the intensity of the band at 5774 cm^{-1} is still related to the intense transitions between the first two rotational levels and corresponds to the hindered tilted vibrator. However, the internal rotational levels $1 < N < 12$ have wave functions localized in a large potential well delimited by the relatively high potential barrier at $\theta = \pm 180°$. They give rise to numerous bands with widespread frequencies oscillating between 5820 and 5740 cm^{-1}, the most intense being around 5774 and 5806 cm^{-1} (corresponding to the "free rotator").

With increasing energy, the overtone spectral patterns become increasingly different from the until-now-known CH overtone spectra of a rotating methyl group. At $\Delta v = 3$, the spectrum exhibits two peaks at 8472 and 8527 and a very weak third peak at 8585 cm^{-1}. At $\Delta v = 4$, only two bands are seen at 11035 and 11140 cm^{-1}. The disappearance of the third higher-energy peak is correlated with the increasingly hindered conformation at $\theta = 180°$. Indeed, at these energies, the effective excited-state potential presents two potential wells around $\theta = \pm 90°$ separated by a potential barrier at $\theta = 0°$, the height of which remains lower than the thermal energy of the molecule (~236 cm^{-1}). These two wells are separated from the two following ones by a potential barrier at $\theta = 180°$, the height of which becomes of the same order of magnitude as the thermal

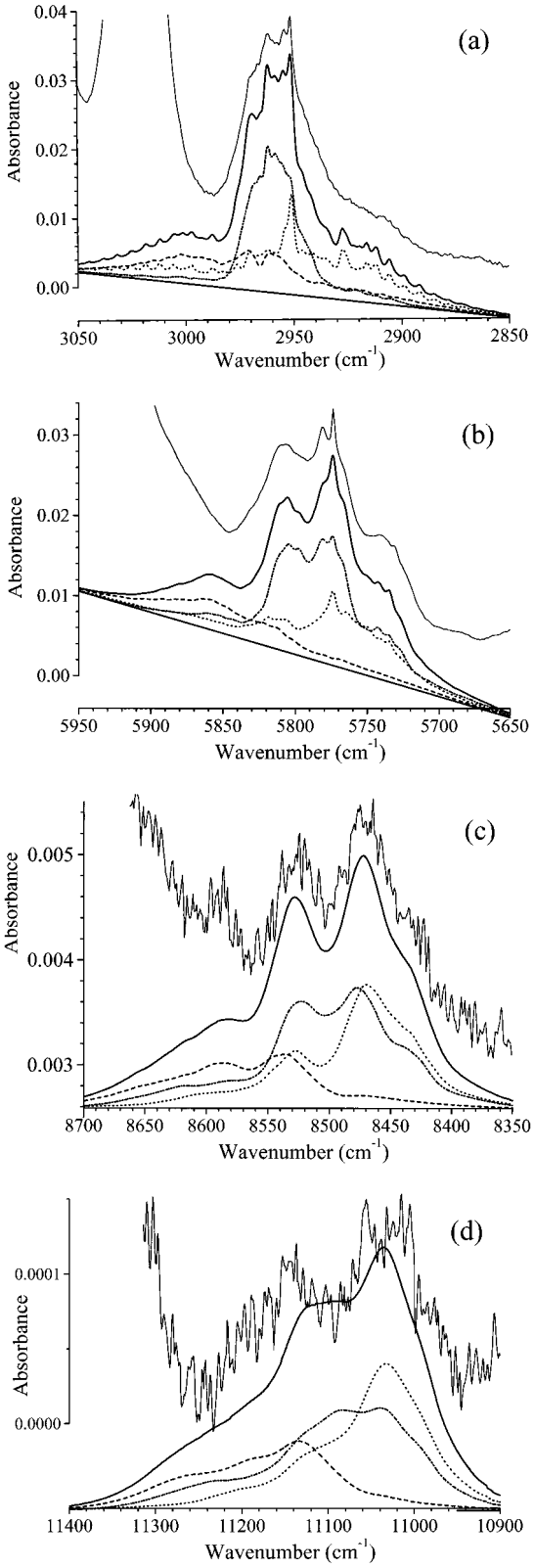

Figure 4. Experimental (top curve) and calculated (next lower curve) FTIR spectra of the CH stretching vibration of gaseous α-picoline-d_2: (a) $\Delta v = 1$, (b) $\Delta v = 2$, (c) $\Delta v = 3$, and (d) $\Delta v = 4$. The calculated spectrum was obtained by summing the contributions of the three dipole moment components (μ_x in dashed lines, μ_y in dotted lines, and μ_z in dash-dotted lines).

energy of the molecule. Most of the intensity of the lower-frequency band is still related to the intense transitions between the first two rotational levels and corresponds to the hindered

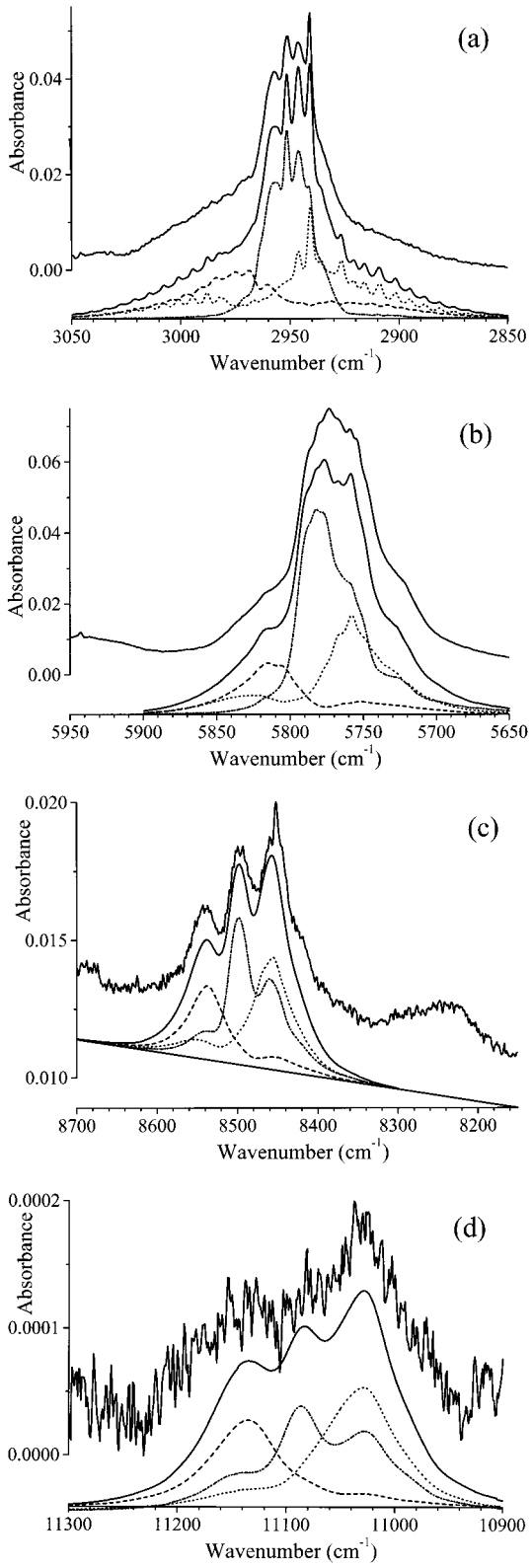

Figure 5. Experimental (top curve) and calculated (next lower curve) FTIR spectra of the CH stretching vibration of gaseous β-picoline-d_6: (a) $\Delta v = 1$, (b) $\Delta v = 2$, (c) $\Delta v = 3$, and (d) $\Delta v = 4$. The calculated spectrum was obtained by summing the contributions of the three dipole moment components (μ_x in dashed lines, μ_y in dotted lines, and μ_z in dash-dotted lines).

tilted vibrator. However, the rest of the spectral features are due to numerous bands with widespread frequencies, corresponding to a vibrator oscillating in a cos θ potential with a relatively high barrier. This also explains the differences noted in the overtone spectra of the CH_3 group of α-picoline by R. Proos and B. Henry,[13] as the effective potentials become increasingly similar for the CHD_2 and CH_3 groups at relatively high energy.[23]

TABLE 5: Ab Initio HF/6-31G Dipole Moment Derivative Expansion Coefficients for the CH Bond in α-Picoline[a]**

$\mu_j'^i(\theta)$	*a*	*b*	*c*	*d*	*e*
$\mu_x'^1$	−0.4967	−0.1109	0.0038	−0.0268	−0.0003
$\mu_x'^2$	−0.8950	−0.0242	0.0450	−0.0409	−0.0086
$\mu_x'^3$	0.0732	0.0181	0.0408	0.0050	−0.0061
$\mu_x'^4$	0.1616	0.0343	0.0615	−0.0097	−0.0706
$\mu_y'^1$	−0.5893	−0.1416	0.0061	−0.0207	−0.0006
$\mu_y'^2$	−1.0665	−0.1129	0.0195	−0.0248	−0.0051
$\mu_y'^3$	0.1295	0.0304	0.0371	0.0063	0.0035
$\mu_y'^4$	0.1308	−0.0429	−0.1315	−0.0260	−0.0514
$\mu_z'^1$	−0.4154	−0.0495	−0.0065	−0.0013	−0.0087
$\mu_z'^2$	−0.8431	−0.0601	0.1632	−0.0019	−0.0094
$\mu_z'^3$	−0.0164	−0.0015	0.1080	0.0014	0.0095
$\mu_z'^4$	0.2217	0.0194	−0.0528	0.0031	0.0038

[a] $\partial^i\mu_j/\partial q^i = \mu_j'^i(\theta) = a + b\cos(\theta) + c\cos(2\theta) + d\cos(3\theta) + e\cos(4\theta)$. The axis $j = x$, y, or z and the derivative $i = 1$, 2, 3, or 4.

TABLE 6: Ab Initio HF/6-31G Dipole Moment Derivative Expansion Coefficients for the CH Bond in *β*-Picoline[a]**

$\mu_j'^i(\theta)$	*a*	*b*	*c*	*d*	*e*
$\mu_x'^1$	−0.5613	−0.0102	−0.0304	0.0017	0.0058
$\mu_x'^2$	−0.9780	−0.0005	0.0319	−0.0038	0.0040
$\mu_x'^3$	0.0606	−0.0149	0.0550	0.0053	0.0050
$\mu_x'^4$	0.1741	0.0049	0.0012	−0.0098	0.0054
$\mu_y'^1$	−0.6570	−0.0066	−0.0339	0.0081	−0.0168
$\mu_y'^2$	−1.1532	−0.0106	−0.0157	0.0063	−0.0267
$\mu_y'^3$	0.1236	−0.0006	0.0515	0.0012	0.0031
$\mu_y'^4$	0.2527	0.0155	0.0293	0.0058	0.0074
$\mu_z'^1$	−0.4725	−0.0154	0.0191	0.0059	−0.0067
$\mu_z'^2$	−0.9109	−0.0191	0.2081	0.0024	−0.0088
$\mu_z'^3$	−0.0406	0.0000	0.1110	−0.0024	0.0097
$\mu_z'^4$	0.2655	0.0027	−0.0643	−0.0035	0.0160

[a] $\partial^i\mu_j/\partial q^i = \mu_j'^i(\theta) = a + b\cos(\theta) + c\cos(2\theta) + d\cos(3\theta) + e\cos(4\theta)$. The axis $j = x$, y, or z and the derivative $i = 1$, 2, 3, or 4.

As we have a pure isotopic compound, the overtone spectra of the aryl CD stretch of β-picoline-d_6 can also be well observed until $\Delta v = 3$ and, with caution, at $\Delta v = 4$, as some overlap with the second overtone spectrum of the aryl CH impurities could occur. These spectra exhibit an intense center peak with two increasingly distinct shoulders as the energy increases. Because of the lower oscillator strength and anharmonicity of the CD stretches leading to smaller band splittings, the analysis of the aryl CD overtone spectra in four components corresponding to the four nonequivalent aryl CD bonds is more difficult to perform than that of the aryl CH overtone spectra.[13] The local-mode bond parameters have been determined from the fitting of these peak frequencies in the same order as was done by R. Proos and B. Henry for the CH vibrators with the following results:[13] C_6D_{10}, $\varpi_0 = 2290 \pm 3$ cm^{-1}, $\bar{\chi} = 34.5 \pm 1$ cm^{-1}; C_4D_9/C_2D_7, $\varpi_0 = 2307 \pm 5$ cm^{-1}, $\bar{\chi} = 33 \pm 2$ cm^{-1}; and C_3D_8, $\varpi_0 = 2325 \pm 2$ cm^{-1}, $\bar{\chi} = 34 \pm 1$ cm^{-1}.

Conclusions

The CH stretching spectra of vapor-phase methylpyridine-2-αd_2,6-d_1, methylpyridine-2-αd_2, and methylpyridine-3-αd_2,-d_4 have been recorded in the $\Delta v_{CH} = 1-4$ region using Raman and FTIR techniques. These spectra display complex band profiles. They have been analyzed from a quantum theory that reflects, in the adiabatic approximation, the coupling of the CH

vibrator with the internal motion. All of the simulated spectra are in good agreement with the experimental ones. This demonstrates the ability of our simple theory to model this means of energy redistribution, which is at the origin of the major part of the complex spectral structure and which indicates the absence of important Fermi resonance until the third overtone in these deuterated molecules.

For both compounds, Raman and fundamental infrared ν(CH) spectra are rather similar to those of toluene-d_7 and γ-picoline-d_7.[11] Nevertheless, some differences between these two groups of molecules can be observed, which can be explained by changes in the type and size of the barrier to internal methyl rotation.

As energy increases, because of the vibrational energy contribution, the effective internal rotational potential is increasingly distorted. For β-picoline, this contribution is very similar to that calculated for toluene-d_7 and γ-picoline-d_7. However, it becomes very different for α-picoline as a consequence of the strong repulsive effect on the methyl CH vibrator of the in-plane lone pair of electrons on the nearby N atom.

At high energy, the methyl CH overtone spectra of β-picoline tend to resemble those of toluene-d_7 and γ-picoline-d_7. The difference in the internal rotational potential is overshadowed by the major vibrational energy contribution to the effective potential in the excited states. For the same reason, the methyl CH overtone spectra of α-picoline exhibit increasingly significant profile changes with increasing energy, which is the signature of the different internal dynamics of the methyl group.

The overtone spectra of the aryl CD stretching of methylpyridine-3-αd_2,-d_4 have also been studied, and their local-mode bond parameters determined.

Acknowledgment. We thank Raymond Cavagnat for the Raman spectra, J.-L. Bruneel for technical assistance, and M. F. Lautié for isotopic compound synthesis.

References and Notes

(1) (a) Seeman, J. I.; Paine, J. B., III; Secor, H. V.; Hoong-Sun, I. M.; Bernstein, E. R. *J. Am. Chem. Soc.* **1992**, *114*, 5269. (b) Seeman, J. I.; Viers, J. W.; Schug, J. C.; Stovall, M. D. *J. Am. Chem. Soc.* **1984**, *106*, 143.

(2) Wiberg, K. B.; Nakaji, D.; Breneman, C. M. *J. Am. Chem. Soc.* **1989**, *111*, 4178.

(3) Del Bene, J. E. *J. Am. Chem. Soc.* **1979**, *101*, 6184.

(4) Draeger, J. A. *Spectrochim. Acta* **1983**, *39A*, 809.

(5) Fan, K.; Boggs, J. E. *Tetrahedron* **1986**, *42*, 1265.

(6) Green, J. H. S.; Kynaston, W.; Paisley, H. M. *Spectrochim. Acta* **1963,** *19*, 549.

(7) Gandolfo, D.; Zarembowitch, J. *Spectrochim. Acta* **1976**, *33A*, 615.

(8) Lamba, O. P.; Parihan, J. S.; Bist, H. D.; Jain, Y. S. *Indian J. Pure Appl. Phys.* **1983**, *21*, 236.

(9) Cavagnat, D.; Lautié, M. F. *J. Raman Spectrosc.* **1990**, *21*, 185.

(10) Bini, R.; Foggi, P.; Della Valle, R. G. *J. Phys. Chem.* **1991**, *95*, 3027.

(11) Lapouge, C.; Cavagnat, D. *J. Phys. Chem.* **1998**, *102*, 8393.

(12) (a) Lopez Tocon, I.; Woolley, M. C.; Otero, J. C.; Marcos, J. I. *J. Mol. Struct.* **1998**, *470*, 241. (b) Arenas, J. F.; Lopez Tocon, I.; Otero, J. C.; Marcos, J. I. *J. Mol. Struct.* **1999**, *476*, 139.

(13) Proos, R. J.; Henry, B. R. *J. Phys. Chem. A* **1999**, *103*, 8762.

(14) Rudolph, H. D.; Dreizler, H.; Seiler, H. Z. *Z. Naturforsch.* **1967**, *22A*, 1738.

(15) Rudolph, H. D.; Dreizler, H.; Mäder, H. Z. *Z. Naturforsch.* **1970**, *25A*, 25.

(16) Cavagnat, D.; Lascombe, J. *J. Mol. Spectrosc.* **1982**, *92*, 141.

(17) Gorse, D.; Cavagnat, D.; Pesquer, M.; Lapouge, C. *J. Phys. Chem.* **1993**, *97*, 4262.

(18) Gough, K. M.; Henry, B. R. *J. Phys. Chem.* **1984**, *88*, 1298.

(19) Sowa, M. G.; Henry, B. R. *J. Chem. Phys.* **1991**, *95*, 3040.

(20) Cavagnat, D.; Lespade, L.; Lapouge, C. *J. Chem. Phys.* **1995**, *103*, 10502.

(21) Kjaergaard, H. G.; Turnbull, D. M.; Henry, B. R. *J. Phys. Chem. A* **1997**, *101*, 2589.

(22) Zhu, C.; Kjaergaard, H. G.; Henry, B. R. *J. Chem. Phys.* **1997**, *107*, 691.

(23) Cavagnat, D.; Lespade, L. *J. Chem. Phys.* **1997**, *106*, 7946.

(24) Cavagnat, D.; Lespade, L. *J. Chem. Phys.* **1998**, *108*, 9275.

(25) Fisch, M. J.; Trucks, G. W.; Head-Gordon, M.; Gill, P. M. W.; Wong, M. W.; Foresman, J. B.; Johnson, B. G.; Schlegel, H. B.; Robb, M. A.; Replogle, E. S.; Gomperts, R.; Andres, J. L.; Raghavachari, K.; Binkley, J. S.; Gonzalez, C.; Martin, R. L.; Fox, D. J.; Defrees, D. J.; Baker, J.; Stewart, J. J. P.; Pople, J. A. *Gaussian 92*, revision A; Gaussian Inc.: Pittsburgh, PA, 1992.

(26) Hollas, J. M. *Recent experimental and computational advances in molecular spectroscopy*; Kluwer Academic Publishers: Dordrecht, The Netherlands, 1993; pp 27−61.

(27) Shu, Q. S.; Campargue, A.; Stoeckel, F. *Spectrochim. Acta* **1994**, *50A*, 663.

(28) Leicknam, J. C.; Guissani, Y.; Bratos, S. *Phys. Rev.* **1980**, *A21*, 1005.

(29) Leicknam, J. C. *Phys. Rev.* **1980**, *A22*, 2286.

(30) (a) Person, W. B.; Newton, J. H. *J. Chem. Phys.* **1974**, *61*, 1040. (b) Gough, K. M.; Srivastava, H. K.; Belohorcová, K. *J. Phys. Chem.* **1994**, *98*, 771. (c) Gough, K. M.; Srivastava, H. K.; Belohorcová, K. *J. Chem. Phys.* **1993**, *98*, 9669.

(31) Cavagnat, D.; Lespade, L., to be published.